Bertolesi, E.; Torres Górriz, B.; Adam, JM.; Calderón García, PA.; Moragues, JJ. (2020). Effectiveness of Textile Reinforced Mortar (TRM) materials for the repair of full-scale timbrel masonry cross vaults. Engineering Structures. 220:1-15. https://doi.org/10.1016/j.engstruct.2020.110978

Effectiveness of Textile Reinforced Mortar (TRM) Materials for the Repair of Full-Scale Timbrel Masonry Cross Vaults

Elisa Bertolesi*, Benjamín Torres, Jose M. Adam, Pedro A. Calderón, Juan J. Moragues.

ICITECH, Universitat Politècnica de València, Camino de Vera s/n, 46022 Valencia, Spain

* Corresponding author: elber4@upv.es

Keyword: Textile Reinforced Mortar (TRM), Timbrel Masonry Cross Vaults, Settlement-Induced Damages, Masonry Strengthening.

Abstract

This paper presents the experimental results obtained from tests on two masonry vaults reinforced by Textile Reinforced Mortar (TRM) materials subjected to monotonic and cyclic vertical settlements in one of their supports. Two full-scale square masonry timbrel vaults were built in one of ICITECH's laboratories at the *Universitat Politecnica de Valencia* (Valencia, Spain) using the traditional Catalan layered-construction technique, with various layers of clay tiles arranged in two perpendicular masonry textures joined by lime and cement mortar joints. Due to their peculiar geometric and mechanical features, i.e. their high slenderness ratio, low tensile strength and high material heterogeneity, these structures are especially prone to damage from high-risk events such as soil settlement or seismic excitation. To evaluate their response to vertical support displacements, both vaults were pre-damaged by either vertical monotonic or cyclic settlements. They were then strengthened by a radial TRM strengthening configuration and re-tested until failure. A complex network of traditional and optical sensors was used to monitor displacements, deformation and the development of the cracking mechanism under both settlement conditions. The results obtained show that TRM materials can be used to effectively repair severely damaged masonry timbrel vaults, helping to partially restore the initial elastic stiffness, as well as doubling the vaults' elastic phase and ultimate displacements. In addition, TRM materials did not alter the stiffness degradation trend, although they had a strong effect on peak reaction degradation and failure modes. This investigation represents a valuable and unique source of information about the efficacy of TRM materials to repair full-scale pre-damaged masonry timbrel vaults.

1. Introduction

Cementitious based strengthening materials, composed of a cement or lime binder, reinforced with continuous long fibers (i.e. TRC, TRM, FRCM), have attracted the attention of the scientific community as an alternative to Fibre Reinforced Polymer (FRP) composites to repair historical masonry structures. Similarly to FRPs, cement-based reinforced-materials are lightweight and easy to apply, whereas conversely to FRPs, they represent an affordable solution because of their low cost, good applicability to irregular and damp surfaces, resistance to high temperatures, good breathability, low invasiveness, and high physical and chemical compatibility with historical structures [3]. Two main types are used, according to the thickness of the reinforcing mortar layer, which is conventionally 30 mm thick [4]. Textile Reinforced Mortar (i.e. TRM) materials, also known as Fibre Reinforced Cementitious Matrix (i.e. FRCM), are thinner, whereas, beyond 30 mm, the cement-based composite is identified as Composite Reinforced Mortar (CRM) or Fibre Reinforced Mortar (FRM). Both types of cement-based composites always contain a heterogeneous mixture of a cement (or lime)-based matrix with limited tensile strength and a reinforcing textile network of continuous long yarns (aramidic, glass, carbon or steel fibres). Unlike FRPs, whose resins ensure a good bond between supports and reinforcements, TRM's adhesive properties may weaken for both microscopic and macroscopic reasons.

From a microscopic point of view, the behaviour of TRM materials is influenced by the friction between: (i) roving filaments and (ii) the grains in the cement matrix and the fibre bundles. The degree of impregnation is closely related to the dimensions of the grains of the inorganic matrix, and the non uniform fibre-to-fibre and fibre-to-matrix load transmissions can easily lead to a "telescopic" failure [3][5]-[9].

From a macroscopic point of view, (as pointed out in [3]) strengthening performance is strongly influenced by four collapse mechanisms: (i) shear failure of the support due to low cohesion, (ii) debonding of the cement strengthening from the substrate, (iii) slippage of the textile in the mortar matrix and (iv) tensile failure of the fibre bundles in the net. The mechanical properties of the substrates play a crucial role, since cement-based composites are often applied to weak masonries. Various studies have been conducted to identify TRM's mechanical properties [5]-[10]. Tensile tests with the application of a pure traction load over rectangular TRM coupons were first employed to analyse their basic behaviour [5]-[11], which turned out to have a tri-linear trend. Other studies assessed the effectiveness of TRM materials applied to isolated structural elements [12]-[16], such as the remarkable example described in [12]. The authors carried out an extensive experimental campaign to evaluate three parameters of the shear performance of various TRM materials applied to square masonry panels: peak tangential strength, shear modulus G and pseudo-ductility. This latter parameter gives important

information on the panels' smooth load decay after the peak load and refers to the ratio between the ultimate shear strain and the shear strain at the yield limit state. The results showed that steel-TRM materials have low tangential strength and G but high ductility, unlike glass-TRM, which exhibited the opposite behaviour. It was also found that premature toe crushing of the masonry could threaten the overall panel performance. Although increasing the strengthening ratio did not prevent failure, it did help to raise ductility. Hair-like cracks propagating along the compressed diagonal until rupture of the reinforcing textile have been reported in several studies [12]-[16]. Deboning phenomena in the crushed toe was the only detaching failure observed in diagonal compression tests, thus reinforcing the idea of the good compatibility of TRM materials and masonry substrates.

Pioneering works on simple and biaxial bending TRM-strengthened panels were analysed in [17][18][19]. [18] studied the effect of coatings and different TRM materials. The coating, which improved the bond between matrix and rovings, raised the peak load to 51% and deformability to 32% in single wythe walls reinforced with one-ply TRM. The enhanced interlocking allowed the panels to exploit the tensile resources of the fibre grid and prevented fibre-to-matrix slippages. Debonding was found only after reaching the maximum load-bearing capacity. In [19], the authors compared the effectiveness of TRM materials in tests on (i) an as-built panel, (ii) a damaged panel reinforced with TRM and (iii) an undamaged TRM-strengthened wall. One layer of basalt-TRM doubled the failure load whether the masonry support was pre-damaged or undamaged. A clear change in the panel failure mechanism was found, making the typical brittle behaviour more ductile and increasing the ultimate displacements at failure by 600%. Slight differences were found between pre-damaged and undamaged TRM-strengthened walls, showing that TRM materials with proper repair techniques are able to restore the original bearing capacity of the panels. Several studies assessed the behaviour of TRM on curved weak masonry supports, including [20]-[23]. The experimental campaign focused on four aspects: (i) cement-based strengthening effectively increased peak loads with respect to their unreinforced counterparts by almost 400% ([23]) in both intrados or extrados configurations, (ii) extrados TRM strengthening showed higher deformation capacity than intrados strengthening (13% and 2% respectively [23]), (iii) the enhancements obtained by higher strengthening ratios are limited by triggering brittle sliding failures, (iv) no debonding failures were found in the extrados of reinforced arches.

Due to their prohibitive cost, few studies have analysed the performance of TRM materials on full-scale structures. [26] studied the dynamic performance of a one-story masonry building tested on a vibrating table and repaired by cement-based materials. The TRM had a double effect on the masonry: (i) it helped to avoid local in- and out-of-plane failures and (ii) forced the masonry to behave as a rigid block. These two aspects are considered positive outcomes of

vulnerability reduction measures. As a matter of fact, a survey of buildings damaged by earthquakes [27][28] found that older buildings often lack: (i) adequate connections between lateral walls, (ii) box behaviour (iii) roof-wall connections. Vaults have been found to be particularly vulnerable [24][29][30] due to their remarkable interaction with their context, so that large differences in lateral stiffness between piers and perimeter walls results in distortions in the supports that have to be absorbed by the masonry vaults.

As no experimental studies have so far analysed the behaviour of TRM materials on full-scale cross vaulted structures, the present work was aimed at filling this gap with a double experimental campaign on full-scale masonry timbrel cross vaults damaged by two types of soil settlement and repaired with TRM materials. The partial collapse of some timbrel vaults in the Church of San Lorenzo de Castell de Cabres in Valencia (Spain) [31] led to the construction and testing of two vaults identical to those that had collapsed, and to analyse the effectiveness of a radial extrados TRM strengthening configuration in restoring the continuity and original load-bearing capacity of severely damaged masonry vaults in a typical damaging scenario.

The paper is organized as follows: Section 2 briefly summarises the geometrical, construction and experimental aspects already described in [1][2] and deals with the novel technique of TRM strengthening. Section 3 presents the displacement protocols and sensor network employed, while Sections 4 and 5 critically review the experimental results and the crack patterns obtained.

2. Experimental Set-up

2.1. Timbrel vault geometry and construction technique

The experimental campaign aimed at evaluating the efficacy of TRM materials on damaged masonry vaulted structures. Two masonry timbrel vaults were built following a typical timbrel construction technique [24][25][31] at the ICITECH laboratories of the Universitat Politecnica de Valencia (Valencia, Spain). The vaults were pre-damaged in a preliminary step by applying two types of vertical movement to one of the supports (see Figure 1). The second step comprised retrofitting with one TRM layer and re-testing the repaired structures by applying monotonic and cyclic vertical settlements (hereinafter identified as Case A and Case B, respectively). The reader is referred to [1][2] for further details on the behaviour of the as-built structures. Both the construction technique and vault geometry were based on the partially collapsed vaults in the Church of San Lorenzo de Castell de Cabres [31], which was used as a reference case study.

The 4x4 m^2 square plan vaults with 1.8 m high lateral arches were built with 230x110x26 mm^3 clay tiles and approximately 10 mm thick mortar joints. Four cubic concrete supports, S1, S2, S3 and S4, were built on steel bases. The arches were composed of a total of seven layers organized into: four layers of clay tiles and three layers of cement mortar, plaster paste and lime mortar joints [1][2]. Construction started with the lateral arches and comprised: (i) one layer of clay tiles and plaster paste, (ii) one layer of cement mortar along the whole arch extrados, (iii) a second layer with clay tiles and cement mortar joints, and finally (iv) a layer of plaster paste. In the second stage, the vaults were built with (v) one layer of clay tiles and plaster paste joints, (vi) one layer of lime mortar and (vii) the last layer of tiles and lime mortar joints overlapping the first. The masonry arrangement was varied by changing the orientation of the two layers of overlapping bricks, as clearly visible in Figure 2-a and 1-b.

2.2. Textile Reinforced Mortar (TRM) strengthening

The strengthening technique was carried out in three phases: (i) injection with a super-fluid injection slurry and masonry assemblage repointing, (ii) application of a 5 mm thick layer of mortar, (iii) placing the fibre glass fabric and (iv) finishing off with the last 5 mm thick mortar layer. Figure 1 highlights (yellow lines), the areas (extrados and intrados) damaged during the previous laboratory campaign, which were repaired by means of the super-fluid slurry. Figure 2 shows some details of the repair interventions carried out to strengthen the two types of vaults, which comprised injection of the extrados and repointing the joints along the intrados and the lateral arches.

Case A		Case B	
Extrados	Intrados	Extrados	Intrados
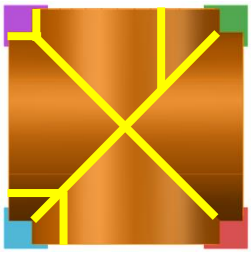	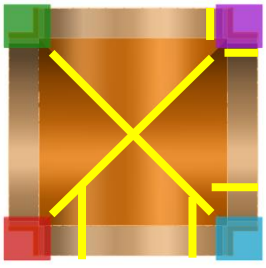	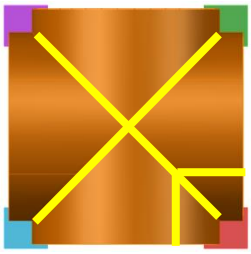	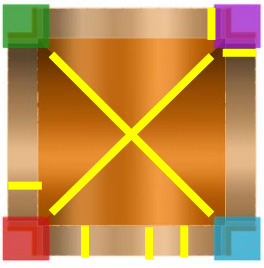

Figure 1: Schematic view of the injections performed on both extrados and intrados of Case A and B vaults.

Case A	Case B
	
-a	-b
	
-c	-d

Figure 2: Injection phases: details of the vaults' extrados (-a and –b) and intrados (-c and –d) with temporary shores to sustain the vaults damaged in the first stage.

The two vaults, Case A and Case B, were strengthened by means of a approximately 10÷15 mm thick layer of TRM material. The glass fibre mesh comprised a 25 mm spacing glass grid with an equivalent resistant area of 35.27 mm^2/m, weight 225 g/mm^2, density 2.5 g/cm^3, ultimate tensile strength 45 kN/m and elastic modulus 72 GPa, according to the manufacturer's specifications [32]. The alkali-resistant fiber mesh was applied to the masonry substrate using a two-component ready-mixed high-ductility fibre reinforced natural hydraulic lime (NHL) and eco-pozzolan based mortar. According to [33], the binder is a Class M mortar characterized by compressive strength at 28 days higher than 15 MPa and Elastic Modulus of 8 GPa.

-a

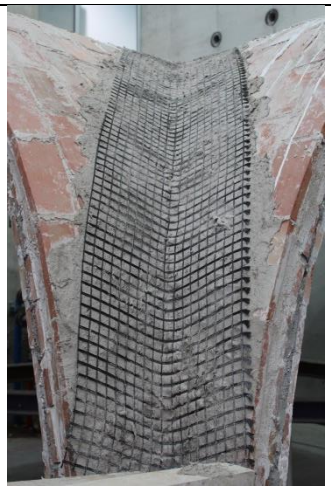

-b

-c

-d

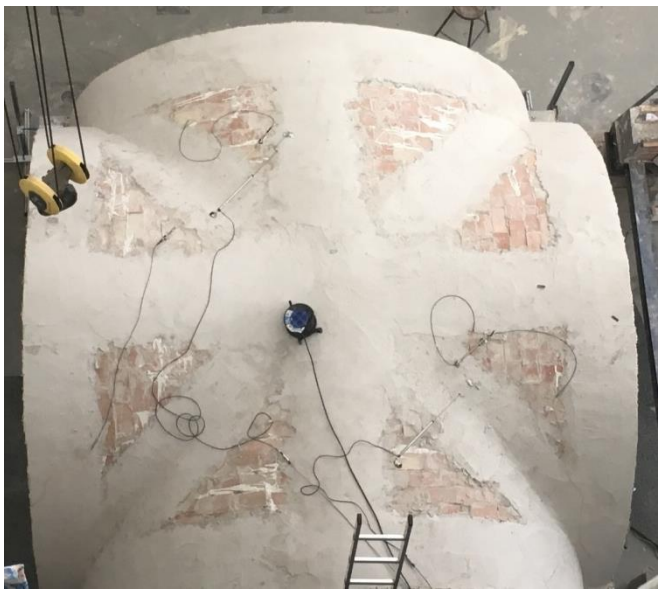

-e

Figure 3: TRM strengthening phases: injection (-a), positioning of diagonal strip (-b), strengthening of lateral arches (-c), detail of the TRM (-d) and final configuration of TRM retrofitting (-e).

Figure 3 depicts the whole strengthening procedure used to repair Case A vault. As can be seen, after the injection phase, the vault extrados was reinforced by 450 mm wide radially placed glass strips. The retrofitting procedure involved applying the strips along: (i) the two diagonal arches (Figure 3-b), (ii) along the four lateral arches (Figure 3-c and -d) and (iii) vertically and horizontally (Figure 3-e). It is worth mentioning that the present study was aimed at evaluating the influence of TRM strengthening materials to re-establish the original continuity of damaged vaults minimizing the invasiveness of the intervention. This implied the preservation of the vault intrados (which in case of historic structures could be characterized by artistic and

architectural values) and designing a realistic repair intervention (i.e. that could be applied on a deformed configuration of the vault). In detail, this strengthening configuration was selected among those discussed in the technical literature, which proposes to strengthen the extrados using: (i) an annular configuration, (ii) a radial configuration and (ii) the whole surface. The first option was excluded since it would have had a negligible influence on the vault' response considering that pre-existent cracks observed at the end of the first investigation opened on the vault extrados along the two principal diagonals and lateral arches (see Figure 1). Similarly, the third configuration was excluded because during the first experimental campaign authors observed that both vaults had a not negligible capacity to accommodate the support movements. The introduction of a stiff continuous layer of TRM material would have dramatically changed the vaults behaviour diminishing their adaptation capacity. Vaults were cured in the laboratory environment for approximately 67 and 33 days for Case A and Case B, respectively. Furthermore, strips were not anchored to the concrete supports, nor were spike anchors or connecting devices used, as clearly visible in Figure 3-d. In agreement with [34], support curvature strongly influences the bearing capacity of reinforcing materials. In fact, intrados repairs are affected by tensile normal stresses which worsen the shear bond performance of the strengthening, anticipating its debonding, whilst in extrados repairs, compressive normal stresses improve bond performance. Connecting devices are thus usually provided only for intrados curved strengthening solutions to absorb the pulling actions derived from the strengthening configuration.

3. Displacement Protocols

Two vertical support distortions were applied to the damaged masonry cross vaults, i.e. a monotonic downward settlement up to 80 mm (Case A) and a cyclical displacement (Case B) comprising a total of 11 half cycles, starting with a downward settlement of 5 mm and gradually doubling the cyclic amplitude until reaching 80 mm. Figure 4 compares the mean value of the vertical settlements applied in the as-built TRM-strengthened vaults for both cases. The vertical settlements were obtained by averaging the displacements recorded by two vertical LVDTs placed between the support S1 and the reaction floor. As clearly visible in Figure 4, both settlements were imposed on the deformed vaults with a residual 40 mm downward displacement in support S1 due to the need to reproduce and analyse in lab conditions the repairs to the damaged masonry cross vaults. As re-establishing the original support positions are costly and time-consuming, in practice it is preferred to improve their structural behaviour and preserve their stability. The following conventions were adopted in the study: positive

relative displacements mean downward settlements, while negative relative displacements refer to upward vertical distortions.

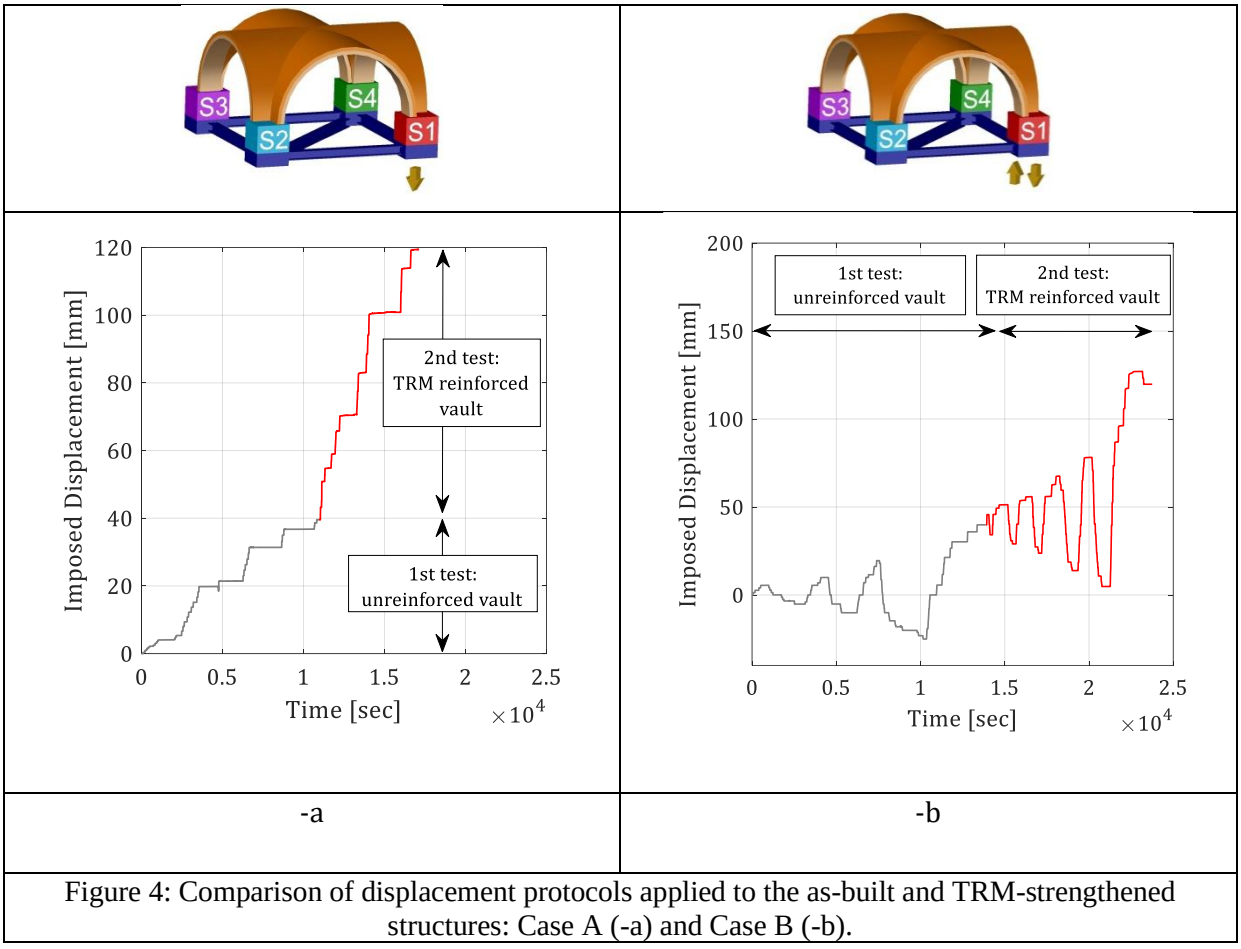

Figure 4: Comparison of displacement protocols applied to the as-built and TRM-strengthened structures: Case A (-a) and Case B (-b).

Both excitations were imposed statically to support S1 (see Figure 5) by means of two manually synchronized mechanical jacks below the steel base. The remaining supports were constrained as follows: support S3 was firmly fixed to the reaction floor. S2 and S4 were only allowed to slide horizontally. Details of the different boundary conditions employed are depicted in Figure 5. A comprehensive description of the laboratory set-up is provided in [1][2], to which the reader is referred for further information.

S2/S4	S1
	

Figure 5: Detail of the boundary conditions of the two tested masonry timbrel vaults.

A steel system composed of 140 mm high HEB girders formed the bracing frame connecting all the supports and providing partial horizontal confinement of the vaults (see Figure 5). The girder frame also helped to avoid excessive diagonal distortions of the vaults by hinging all the steel bases and allowed the positioning of three load cells to monitor vertical reactions in supports S1, S2 and S4. Displacements and deformations were tracked by means of Linear Displacement Variable Transducers (LVDTs) and Optical Sensors (FOS), respectively (see Figure 6). Crack patterns and abrupt changes in the vaults' behaviour were detected by recurring visual inspections during the lab tests.

-a

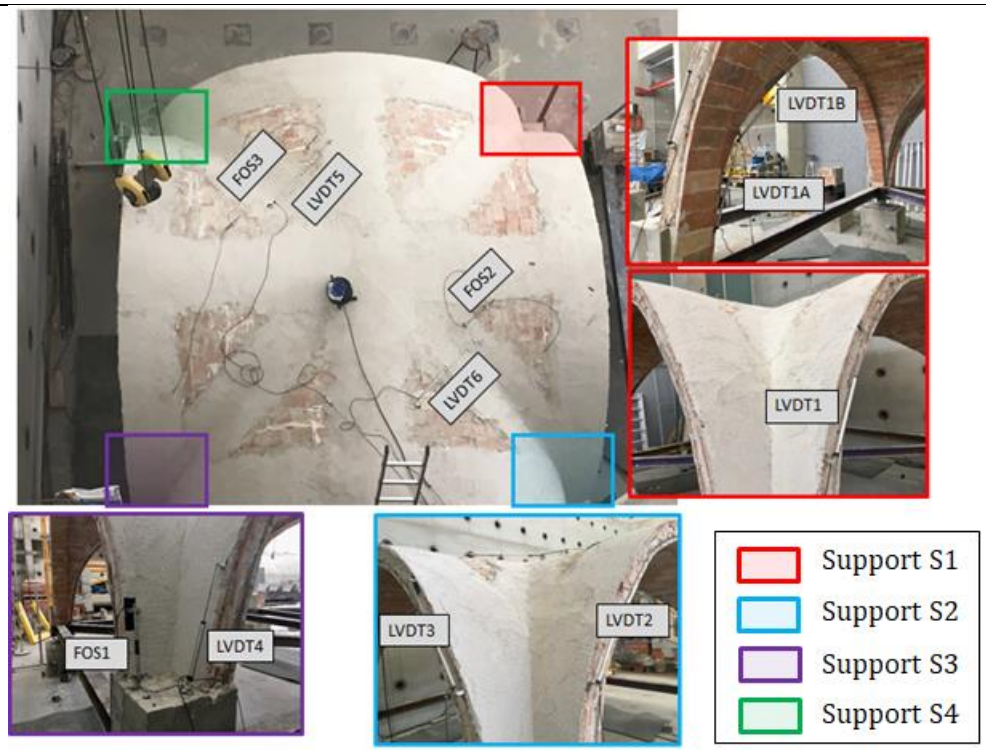

-b

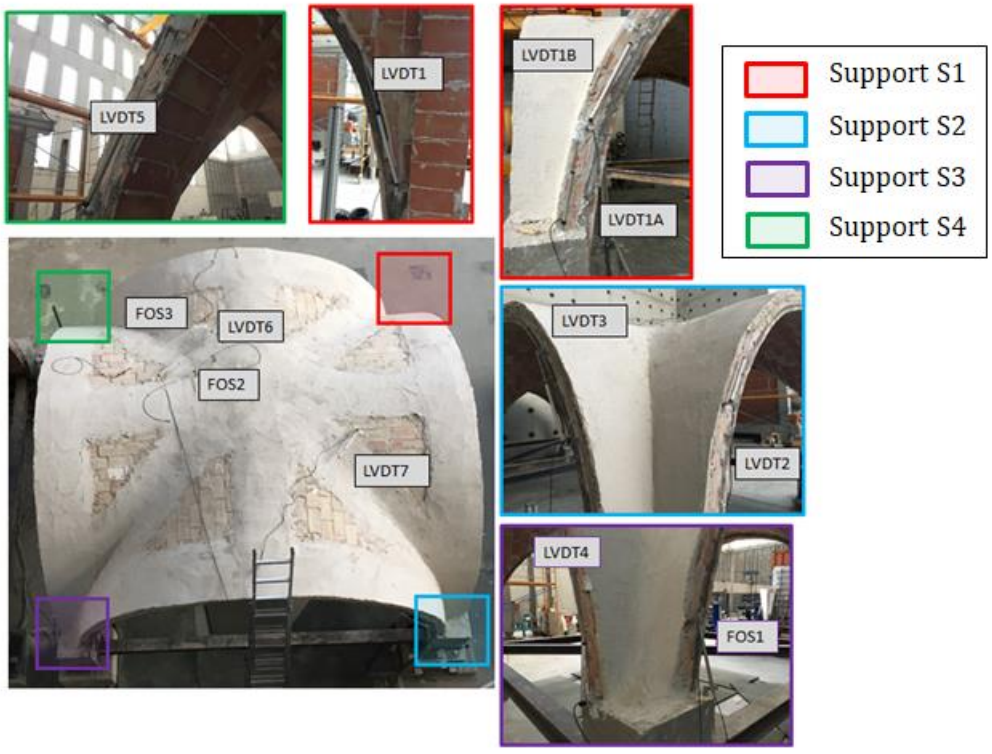

Figure 6: Network of LVDTs and optical sensors used to monitor displacement and deformations during the tests: Case A (-a) and Case B (-b).

4. Experimental Results

The aim of this and the next sections is to demonstrate the effectiveness of TRM repair materials by comparing the strengthened vault's behaviour with that of the unreinforced counterparts described in [1][2]. The structural response of the vault is analysed after applying a monotonically increased settlement (Case A) in Section 4.1, while Section 4.2 presents the results of the TRM-strengthened vault subjected to cyclic movements (Case B). Stiffness and strength degradations were considered a straightforward way of evaluating TRM performance and comparing it to the unreinforced case. Envelope curves were deduced from the cyclic reaction force – displacement curves and compared to those of Case A with and without reinforcing materials.

4.1. Monotonic settlement

Figure 7-a depicts the reaction force-displacement curves obtained experimentally in supports S1, S2 and S4 (Case A).

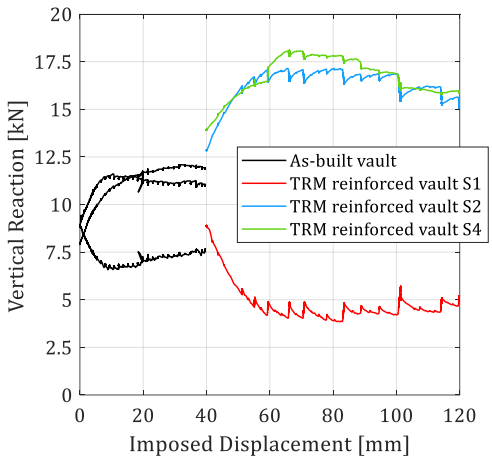

-a

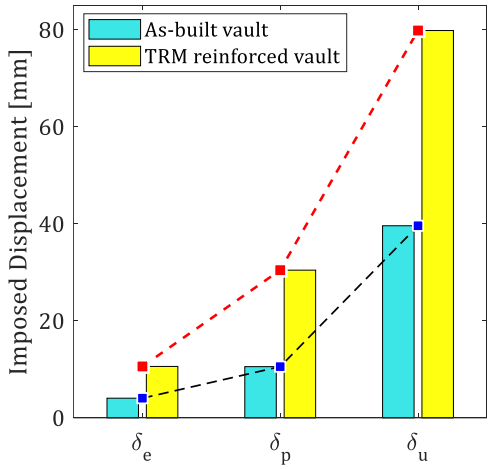

-b

Figure 7: Reaction forces vs imposed displacement curves (Case A) obtained experimentally(-a) and displacement capacity comparison (-b).

As can be seen in Figure 7-a, the vaults behaviour can be divided into three phases: (i) the initial elastic response was obtained up to 10 mm, (ii) from 10 mm to 30 mm, behaviour was non-linear until the peak reaction value (Rp), and (iii) in the third phase a negligible reduction of the reaction forces was observed up to failure at 80 mm. Further results are provided in Figure 7-b and Figure 8. Figure 7-b compares the displacements reached by the as-built and TRM strengthened timbrel vaults : (i) at the end of the elastic phase (δe), (ii) at peak reaction forces (δp), and (iii) at failure (δu). The TRM had a twofold effect: (i) it helped to extend the elastic

phase, which doubled (from 5 mm to 10 mm) and the vault displacement capacity, (ii) it considerably delayed the vault failure, which occurred at 80 mm, instead of 40 mm as happened for the as-built structure.

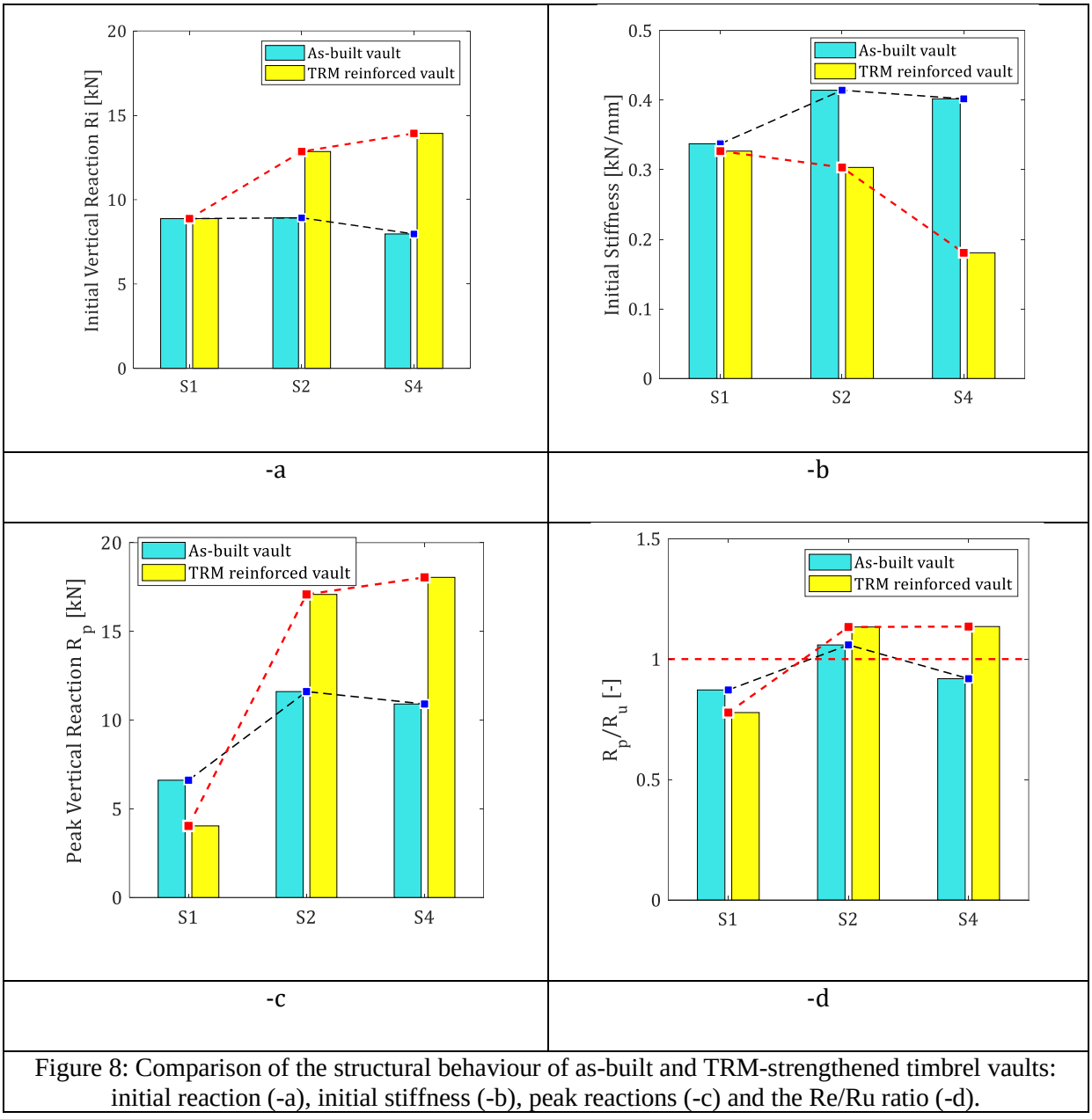

Figure 8: Comparison of the structural behaviour of as-built and TRM-strengthened timbrel vaults: initial reaction (-a), initial stiffness (-b), peak reactions (-c) and the Re/Ru ratio (-d).

Figure 8-a compares the vertical reaction forces (Ri) at the beginning of the tests on the unreinforced and TRM-strengthened vaults. Apart from a few differences, the initial reactions of the TRM-strengthened vault are similar to those monitored at the end of the unreinforced vault test. Considering the as-built structure, there are negligible differences between the three reaction values in all the monitored supports, confirming an approximately equal re-distribution of the vault's weight. Conversely, the second test was performed starting from the deformed vault configuration obtained at the end of the first test and then applying the monotonic settlement. As expected, since the test started with a downward residual

displacement of 40 mm in support S1, the equal distribution of the reaction forces in the as-built structure was altered, especially in the initial reactions (Ri) in S2 and S4, which increased almost symmetrically. Unexpectedly, the reaction force in S1 was not altered by the initial deformed vault configuration.

Figure 8-b depicts the initial stiffness values calculated as the slope of the vaults' elastic response (until 5 mm for the as-built and 10 mm for the TRM-strengthened vaults) of all the monitored supports. The TRM helped re-establish the original stiffness in S1, while a slightly reduction was observed in supports S2 and S4. A different trend was found after analysing the influence of TRM materials on the peak reaction forces throughout the test. A comparison of the response of the as-built and repaired structures is given in Figure 8-c. As discussed above, TRM strengthening materials extended the vault elastic phase and delayed its failure. This phenomenon influenced the peak reaction forces. Indeed, due to the extension of the vault displacement capacity produced by the application of the TRM material, a higher vertical reaction unloading phase was observed in support S1, which was accompanied by a consequent increase in the vertical reactions in supports S2 and S4. This behaviour was also observed in the as-built structure (see Figure 8-c) even if the premature formation of the cracking mechanism interrupted the redistribution of the vertical loads into the vault supports. Figure 8-d depicts the ratio between the peak reaction forces (Rp) at 10 mm (as-built vault) and 30 mm (TRM vault) and their ultimate values at collapse (Ru). As clearly visible, both unreinforced and reinforced vaults showed a post-peak softening behaviour characterized by a slight reduction of the reaction forces at failure.

4.2. Cyclic settlement

This section describes the experimental results obtained after applying a cyclic vertical movement to support S1 in the second vault (Case B). Several analyses compared the cyclic responses of the as-built and TRM strengthened vaults, as shown in Figure 9, Figure 10 and Figure 11. Figure 9 depicts the reaction force-displacement curves obtained in supports S1, S2 and S4. The curves are traced in the same colour as the corresponding support numbers and superimposed on the unreinforced counterparts. A more detailed analysis of the effect of TRM materials is shown in Figure 10, which gives the stiffness and strength degradation values obtained, calculated as in [2]. Elastic stiffness degradation was computed as the slope of the force-displacement curves monitored in all the cycles of the lab investigation up to 80% of the peak reaction forces.

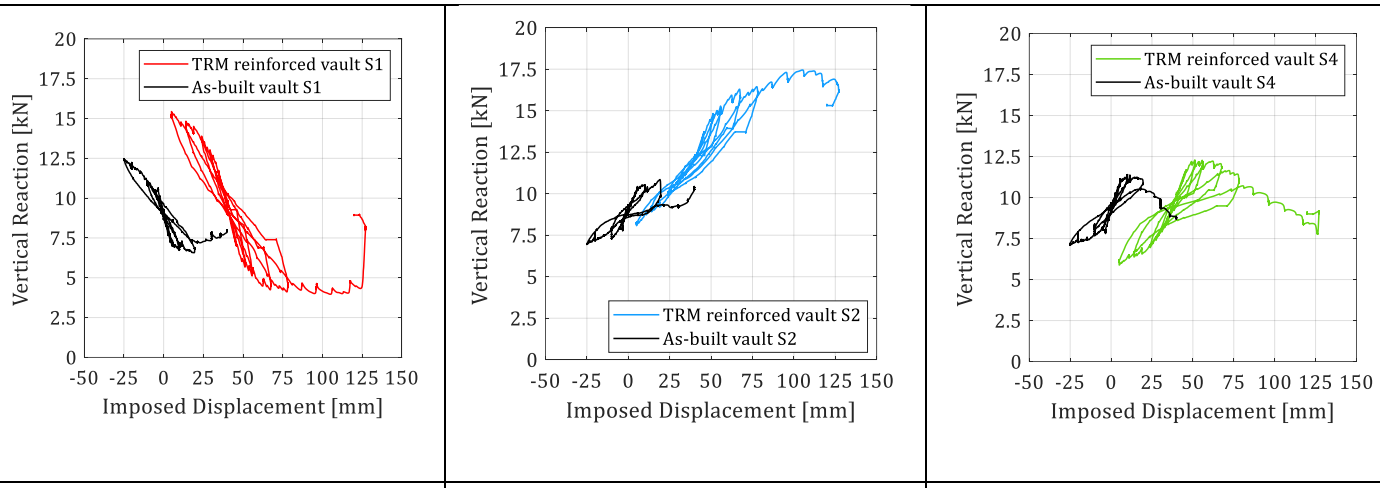

-a -b -c

Figure 9: Reaction force-displacement curves (Case B) in supports: S1 (-a), S2 (-b) and S4 (-c).

As expected, in the TRM-strengthened vault the initial elastic stiffness progressively degraded up to a maximum of four times at 80 mm in support S1. As in the unreinforced case, this behaviour was due to the triggering of a progressive damage mechanism, which will be discussed in the next section. The initial stiffness values in the first cycle (Case B cyclic) (see Figure 10-a) were quite similar to those of the undamaged unreinforced vault (Case B cyclic) at the beginning of the test and to those of Case A shown in Figure 8-c.

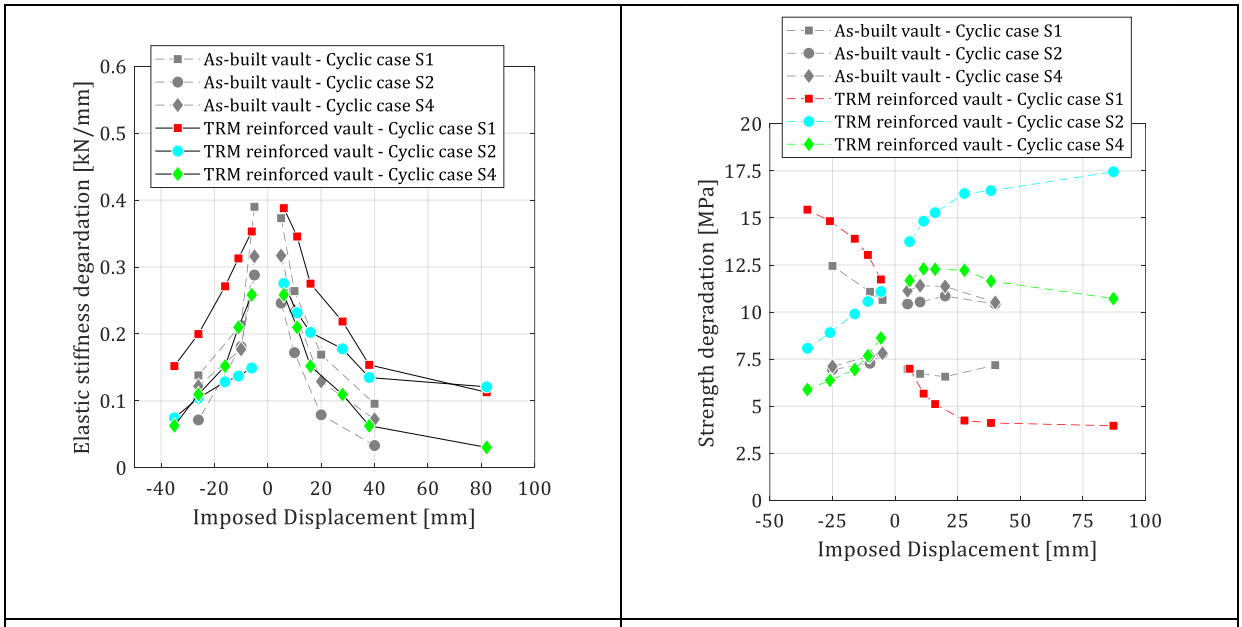

-a -b

Figure 10: Stiffness (-a) and strength degradation (-b) of unreinforced and TRM-strengthened vaults in Case B.

Although negligible differences were detected due to material heterogeneity, the consistency of the values from the beginning of the test confirmed the effectiveness of TRM in recovering the structure's original stiffness (see Figure 10-a). Strength degradation is another important parameter (Figure 10-b). The strength degradation curves were drawn using the peak reaction forces obtained in each cycle of all the monitored supports. As can be seen in Figure 10-b, the TRM strengthening changed the unreinforced vault's strength degradation trend found in [2]. Unexpectedly, both up and down movements showed a clear increasing trend common to all the supports in all cycles, except for the last cycles. Theoretically, due to the symmetry axis connecting supports S1-S3, the structural response of support S4 should be similar to S2. This behaviour was completely lost in support S4, which evidenced a different trend (see Figure 10-b). The obtained behaviour could be justified by the asymmetric cracking mechanism which forced the vault to evidence not negligible torsional effects. The effect of the induced torsion was to increase the gravity load on support S2, while decreasing the reaction forces in his symmetric counterpart S4. From a general point of view, the TRM-strengthened vault's behaviour was quite symmetric under upward and downward settlements. However, the slope of the strength degradation curve abruptly changed in all the supports after 40 mm, meaning that the triggered collapse mechanism was about to threaten vault stability.

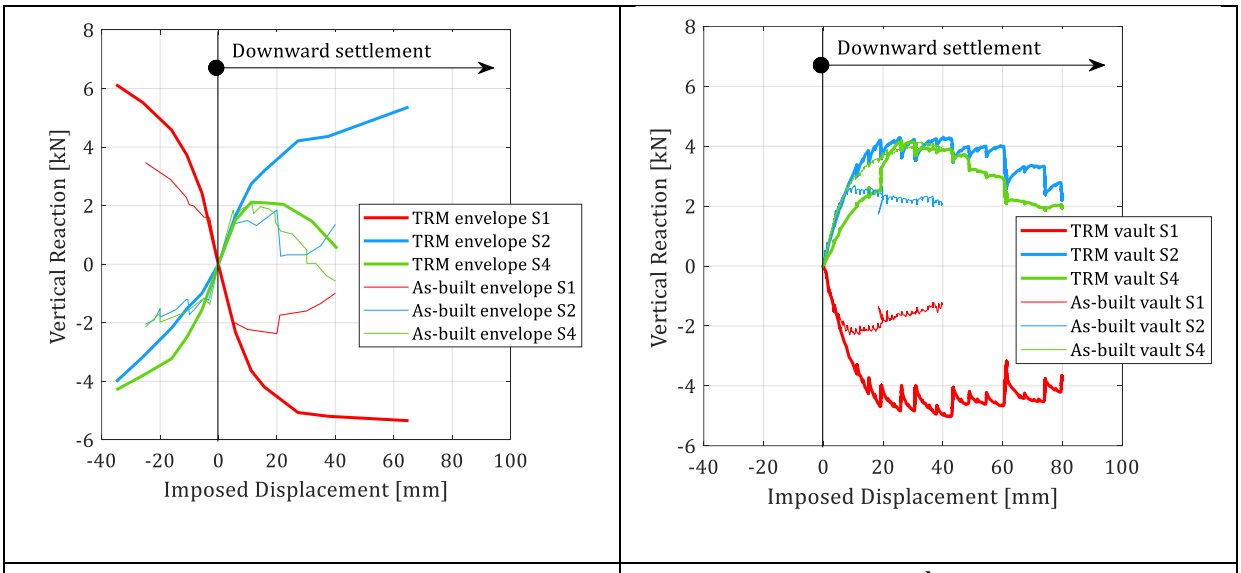

-a -b

Figure 11: Comparison of as-built and TRM vaults' Case B envelopes (-a) and Case A (-b).

Figure 11-a compares the envelope curves obtained from the unreinforced and TRM-strengthened vaults in Case B, while Figure 11-b gives the increments in the reaction force-displacement curves obtained in the as-built [1] and TRM-strengthened vaults (Case A). For the as-built vault [2] (Figure 11-a), the envelope curves were constructed starting from the peak

forces obtained during the cyclic settlement and the corresponding displacements imposed in each cycle. Theoretically, the curves so obtained can be used to estimate the vault behaviour with either up or down movements. It is thus particularly interesting to compare the envelopes of the downward movements shown in Figure 11-a to those in Figure 11-b, which confirm the previous findings on TRM materials. This type of reinforcement allowed the vaults to: (i) almost fully recover the vaults' initial elastic stiffness, (ii) double the elastic phase of the structures and (iii) double the displacement capacity at failure.

5. Crack patterns

5.1. Monotonic settlement

This section deals with the crack patterns in the Case A TRM-strengthened vault. At the end of the first test (unreinforced vault subjected to monotonic settlement) [1], two different crack patterns were observed: (i) cracks formed in mortar joints close to supports S1 and S3 and in some damaged bricks in S2, (ii) a diagonal curved hinge crack opened on the vault extrados and propagated along the diagonal arch connecting S2 and S4. Due to the low tensile strength of the masonry assembly, the crack (ii) spread to the whole section. As vault stability was seriously threatened, the authors decided to stop the test and carry out repairs. Despite the injections, the TRM-strengthened vault experienced: (i) the opening of one extrados curved hinge connecting supports S2-S4 and (ii) traditional hinge mechanisms in the lateral arches. Extrados strengthening configurations are able to delay the formation of cracks and increase the tensile strength of the support where the reinforcement is applied. Conversely, weaker areas, such as those repaired by repointing, are much more vulnerable to damage mechanisms. For this reason, the LVDTs were placed close to the cracked areas in the unreinforced vault. Figure 12-Figure 15 depict the cracking mechanisms in the supports at the end of the tests. Figure 12 shows the observed cracks on the lateral arches connected to support S3.

-a | -b | -c

Figure 12: Cracking mechanism in support S3: lateral arch S4-S3 (-a), lateral arch S3-S2 (-b) and support S3 front view (-c).

Hinges were also detected near S2 and S4, as shown in Figure 13 and Figure 14, respectively. The cracks in the extrados (Figure 13) were in the reinforcing mortar. No debonding or fibre-to-matrix slippages were detected during the whole series of tests. The activated damage mechanism affected the reinforcing mortar matrix but there was no tensile failure of the glass grid.

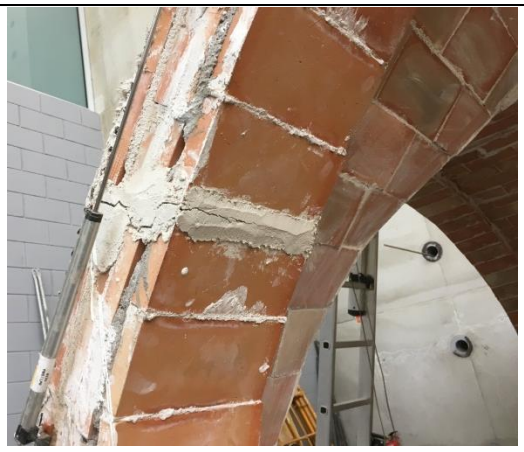

-a | -b

Figure 13: Cracking mechanism in support S2: crack formation in lateral arch S2-S1 (-a) and support S2 front view (-b).

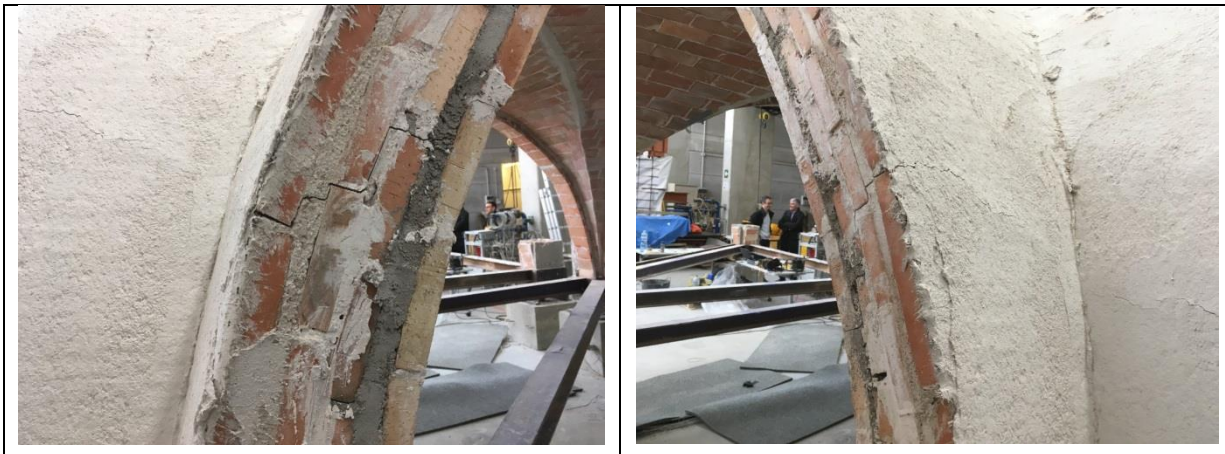

-a -b

Figure 14: Cracking mechanism in support S4: lateral arch S4-S3 (-a) and lateral arch S4-S1 (-b).

It should be noted that the cracks on lateral arches S4-S1 and S2-S1 attempted to join up with the diagonal hinge between supports S2-S4. This peculiar failure mechanism also occurred in the unreinforced vault [1] (Figure 15). This behaviour was monitored by the sensor network. Figure 16 gives the displacement read by the LVDTs on the unreinforced vault (between 0 to 40 mm) and the TRM-repaired vault (between 40 to 120 mm). In support S1, maximum displacements ranged from 0.05 mm in the unreinforced to 0.15 mm in the reinforced vault. LVDT 2 and LVDT 3 detected two cracks with maximum openings of 3-4 mm in support S2 (Figure 13). LVDT 4 (Figure 12-c) captured a maximum displacement of 4.5 mm, again in agreement with the crack pattern previously described. LVDT 5 monitored the formation of the hinged diagonal crack along supports S2-S4 on the vault extrados, which doubled in size from 2.5 mm in the unreinforced case to 5 mm in the reinforced vault. This again confirms the ability of TRM materials to extend masonry displacement capacity and delay failure.

-a -b

Figure 15: Cracking mechanism in support S1: lateral arch S1-S2 (-a) and intrados view of diagonal arch S3-S1 (-b).

355

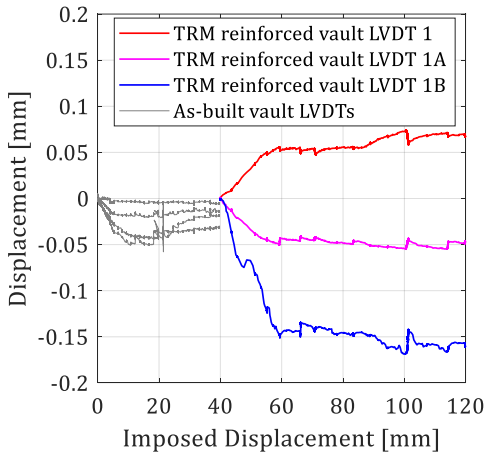

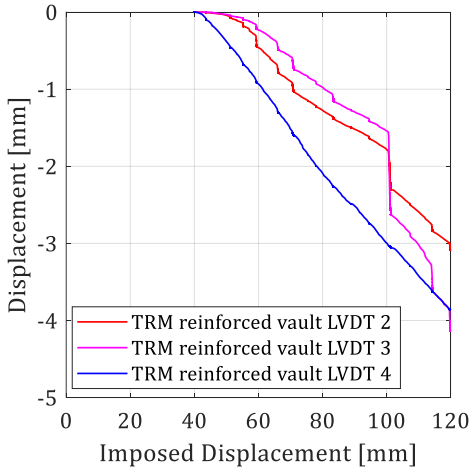

-a -b

-c

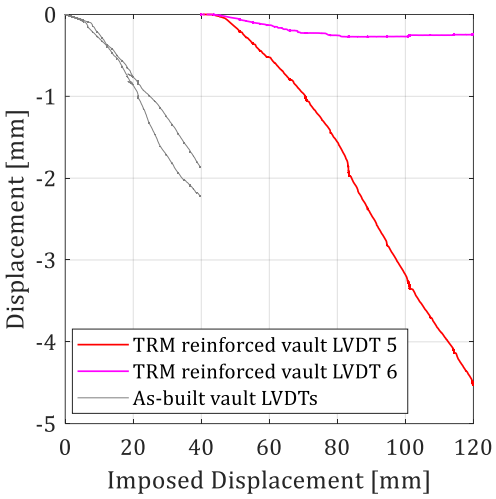

Figure 16: Displacements (Case A) recorded by the most important LVDTs: in S1 (-a), in S2 and S3 (-b) and on the vault extrados (-c).

5.2. Cyclic settlement

Similarly to the monotonic case, the TRM-strengthened vault subjected to cyclic settlements (Case B) experienced the formation of hinges in the lateral arches and the widening of a diagonal crack on arch S2-S4. Alternate displacements led to complex damage patterns with cracks along the vault extrados and intrados.

-a

-b

Figure 17: Cracking mechanism in support S3: detail of the support (-a) and crack in the lateral arch S3-S2 close to S2 (-b).

Figure 17 shows the cracks on support S3 and along the lateral arch S3-S2. LVDT 4 tracked the separation of abutment S3 from the concrete support, which reached a maximum opening of 7 mm (Figure 18-a.) Figure 18-a also depicts the displacements recorded by the LVDTs close to supports S2-S3 and S4 during the testing of the unreinforced vault. The cracks formed during the first test were relatively narrow (3 mm). In the reinforced vault severe damage was detected on the extrados and intrados of support S2 (see Figure 19-a). A deep crack formed close to support S2 during upward movements. LVDTs 2 and 3 detected the second damage mechanism shown in Figure 17-b and Figure 19-b. Both lateral arches S2-S1 and S2-S3 experienced wide cracks on the extrados which affected the vault's integrity, those on the former arch opening up to approximately 16 mm.

At this point, the TRM experienced preliminary cracking of the reinforcing mortar, followed by the progressive tensile failure of the glass grid. The same thing happened in lateral arch S2-S3. In this case, the crack, which propagated across the mortar joints, caused the external layers of masonry to separate. Although a visual inspection showed the crack was similar to the one in arch S2-S1, LVDT 3 could only partially detect it.

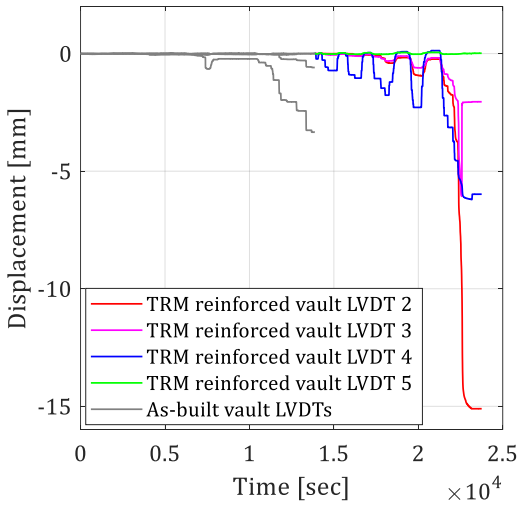

-a

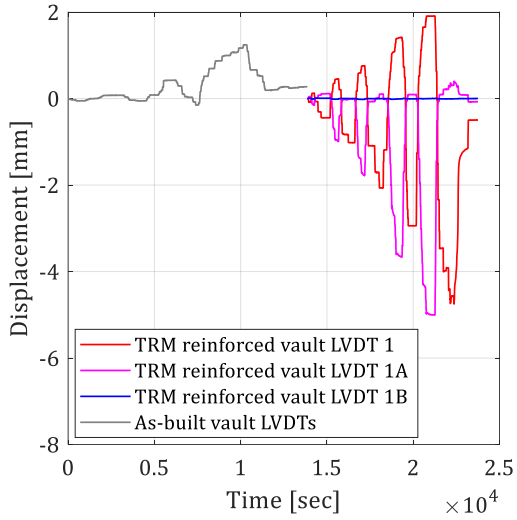

-b

-c

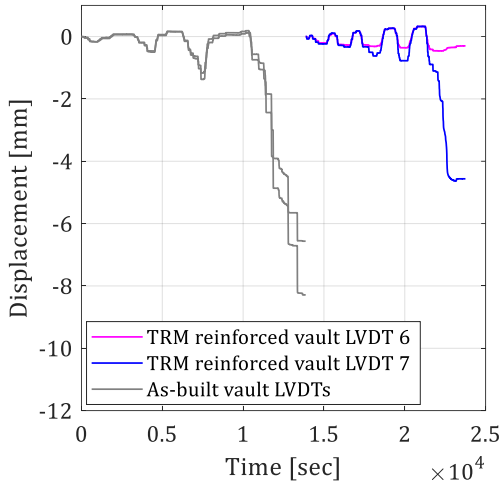

Figure 18: Displacements (Case B) recorded by the most important LVDTs in S2, S3 and S4 (-a), in S1 (-b), and on the vault extrados (-c).

376 Similar cracks with lower displacement values were detected in support S1, as shown in Figure
377 18-b and Figure 20-a.

-a

-b

Figure 19: Cracking mechanism in support S2: support intrados (-a) and extrados (-b).

378

-a

-b

Figure 20: Cracking mechanism in support S1: detail of intrados (-a) and general view (-b).

Figure 18-c depicts the LVTDs placed along the vault extrados. Only one LVDT tracked the formation of the diagonal hinge that opened between supports S2-S4 on both extrados and intrados due to the cyclic settlement (Figure 20-b). As in Case A, a maximum value of 5 mm was detected on the extrados. Unlike the unreinforced case (Case B), the TRM avoided the premature separation of the vault into two independent parts (Figure 21). Figure 21 compares the crack patterns at the end of the cyclic test in the reinforced and unreinforced vaults. The cracks on the extrados were diverted by the reinforcing materials to the masonry away from the retrofitted zones. The TRM radial configuration prevented the crack on the top of the extrados from propagating. This effect is particularly evident in Figure 18-c. The cracks reached a maximum value of 8 mm at the end of the test in the unreinforced vault, or approximately half the width of the opening in the reinforced vault.

-a -b

Figure 21: Comparison of Case B vault cracking patterns: unreinforced (-a) and reinforced vault (-b).

6. Conclusions

This paper analysed the effectiveness of radial TRM strengthening configurations for the repair of two pre-damaged masonry timbrel cross vaults subjected to different vertical support movements. The lab tests comprised the application of monotonic (Case A) and cyclic (Case B) settlements in one of the vault supports. The method adopted showed the validity and limitations of TRM repair materials by comparing the behaviour of the strengthened and unreinforced vaults. The repair technique was evaluated in terms of: (i) the reaction force-imposed displacement curves obtained at the end of the tests, (ii) cracking patterns and (iii) crack widths. Future research will be devoted to the evaluation and comparison of the experimental results by means of advanced numerical modelling.

The results obtained allow us to draw the following conclusions:

- The paper describes a repair technique to be used for severely damaged masonry cross vaults composed of: injection, masonry repointing and application of TRM materials in a radial pattern on the extrados.
- TRM materials restored the continuity of two severely damaged timbrel cross vaults.
- The proposed radial strengthening configuration partially restored the initial elastic stiffness of the damaged vaults in both cases.
- TRM strengthening doubled the vaults' elastic phase and ultimate displacements.
- TRM materials did not alter the stiffness degradation trend, although they had a strong effect on peak reaction degradation.
- In the cyclic tests the TRM-repaired vault sustained much more serious damage than at the end of the monotonic tests. For example, support S2 had a maximum crack opening of 16 mm.
- TRM failure in Case A (monotonic downward settlement) comprised the cracking of the reinforcing mortar. No debonding, fibre-to-matrix slippage or tensile failures of the textile grid were detected.
- TRM failure in Case B (cyclic vertical movement) was characterized by the opening of wide cracks in support S2, with the cracking of the mortar matrix and tensile failure of the glass grid.

7. References

[1] B. Torres, E. Bertolesi, J.J. Moragues, P.A. Calderón, J.M. Adam, Experimental investigation of a full-scale timbrel masonry cross vault subjected to vertical settlement, Construction and Building Materials, v. 221 (2019), pp. 421-432.

[2] B. Torres, E. Bertolesi, P.A. Calderón, J.J. Moragues, J.M. Adam, A full-scale timbrel cross vault subjected to vertical cyclical displacements in one of its supports, Engineering Structures, v. 183 (2019), pp. 791-804.

[3] L. Alexandros, S.K. Thanasis, C. Triantafillou, State-of-the-art on strengthening of masonry structures with textile reinforced mortar (TRM), Construction and Building Materials, v. 188(2018), pp. 1221-1233.

[4] M. Del Zoppo, M. Di Ludovico, A. Balsamo, A. Prota, In-plane shear capacity of tuff masonry walls with traditional and innovative Composite Reinforced Mortars (CRM), Construction and Building Materials, v. 210 (2019), pp. 289-300.

[5] F.G. Carozzi, A. Bellini, T. D'Antino, G. de Felice, F. Focacci, Ł. Hojdys, L. Laghi, E. Lanoye, F. Micelli, M. Panizza, C. Poggi, Experimental investigation of tensile and bond properties

436 of Carbon-FRCM composites for strengthening masonry elements,Composites Part B:
437 Engineering, v. 128 (2017), pp. 100-119.
438 [6] M. Leone, M.A. Aiello, A. Balsamo, F.G. Carozzi, F. Ceroni, M. Corradi, et al.,Glass fabric
439 reinforced cementitious matrix: tensile properties and bond performance on masonry
440 substrate, Compos Part B-Eng, v. 127 (2017), pp. 196-214.
441 [7] C. Caggegi, F.G. Carozzi, S. De Santis, F. Fabbrocino, F. Focacci, L. Hojdys, et al.,
442 Experimental analysis on tensile and bond properties of PBO and Aramid fabric
443 reinforced cementitious matrix for strengthening masonry structures, Compos Part B-
444 Eng, v. 127 (2017), pp. 175-195.
445 [8] C. Caggegi, E. Lanoye, K. Djama, A. Bassil, A. Gabor, Tensile behaviour of a basalt TRM
446 strengthening system: influence of mortar and reinforcing textile ratios, Compos. Part B
447 Eng., v. 130 (2017), pp. 90-102.
448 [9] L. Ascione, G. De Felice, S. De Santis, A qualification method for externally bonded Fibre
449 Reinforced Cementitious Matrix (FRCM) strengthening systems, Compos. Part B Eng., v.
450 78 (2015), pp. 497-506.
451 [10] E. Bertolesi, F.G. Carozzi, G. Milani, C. Poggi, Numerical modeling of Fabric Reinforce
452 Cementitious Matrix composites (FRCM) in tension, Construction and Building
453 Materials, v. 70 (2014), pp. 531-548.
454 [11] L.H. Sneed, T. D'Antino, C. Carloni, C. Pellegrino, A comparison of the bond behavior of
455 PBO-FRCM composites determined with double-lap and single-lap shear tests, Cem
456 Concr Compos, v. 64 (2015), pp. 37-48.
457 [12] X. Wang, C.C. Lam, V. PanIu, Comparison of different types of TRM composites for
458 strengthening masonry panels, Construction and Building Materials, v. 219, (2019), pp.
459 184-194.
460 [13] F. Parisi, I. Iovinella, A. Balsamo, N. Augenti, A. Prota, In-plane behaviour of tuff masonry
461 strengthened with inorganic matrix-grid composites, Composites Part B: Eng., 45
462 (2013), pp. 1657-1666.
463 [14] C. Faella, E. Martinelli, E. Nigro, S. Paciello, Shear capacity of masonry walls externally
464 strengthened by a cement-based composite material: An experimental campaign, Constr.
465 Build. Mater., 24 (2010), pp. 84-93.
466 [15] N. Augenti, F. Parisi, A. Prota, G. Manfredi, In-plane lateral response of a full-scale
467 masonry sub-assemblage with and without an inorganic matrix–grid strengthening
468 system, J Compos Constr, 15 (2011), pp. 578-590.
469 [16] L. Garmendia, P. Larrinaga, R. San-Mateos, J.T. San-Jose, Strengthening masonry vaults
470 with organic and inorganic composites: an experimental approach, Mater. Des., 85
471 (2015), pp. 102-114.

[17] N. Ismail, J.M. Ingham, In-plane and out-of-plane testing of unreinforced masonry walls strengthened using polymer textile reinforced mortar, Eng. Struct., v. 118 (2016), pp. 167-177.

[18] F.A. Kariou, S.P. Triantafyllou, D.A. Bournas, L.N. Koutasc, Out-of-plane response of masonry walls strengthened using textile-mortar system,Construction and Building Materials, v. 165, (2018), pp. 769-781.

[19] C. D'Ambra, G.P. Lignola, A. Prota, E. Sacco, F. Fabbrocino, Experimental performance of FRCM retrofit on out-of-plane behaviour of clay brick walls, Composites Part B, v. 148 (2018), pp. 198-206.

[20] F.A. Kariou ,S.P. Triantafyllou, D.A. Bournas, TRM strengthening of masonry arches: An experimental investigation on the effect of strengthening layout and textile fibre material, Composites Part B, v. 173, (2019), pp. 106-

[21] V. Giamundo, G.P. Lignola, G. Maddaloni, A. Balsamo, A. Prota, G. Manfredi, Experimental investigation of the seismic performances of IMG reinforcement on curved masonry elements, Composites: Part B, v. 70, (2015), pp. 53–63.

[22] L. Garmendia, J.T. San-José, D. García, P. Larrinaga, Rehabilitation of masonry arches with compatible advanced composite material, Construction and Building Materials, v. 25, (2011), pp. 4374–4385.

[23] V. Alecci, G. Misseri, L. Rovero, G. Stipo, M. De Stefano, L. Feo, R. Luciano, Experimental investigation on masonry arches strengthened with PBO-FRCM composite, Composites Part B, v. 100, (2016), pp. 228-239.

[24] E. Bertolesi, J. M. Adam, P. Rinaudo, P. A. Calderón, Research and practice on masonry cross vaults – A review, Engineering Structures, v. 180 (2019), pp. 67-88.

[25] M. Angelillo, Static analysis of a Guastavino helical stair as a layered masonry shell, Composite Structures, v. 119, (2015), pp. 298-304.

[26] G. Maddaloni, M. Di Ludovico, A. Balsamo, G. Maddaloni, A. Prota, Dynamic assessment of innovative retrofit techniques for masonry buildings, Composites Part B: Engineering, v. 147, (2018), pp. 147-161.

[27] F. Parisi, N. Augenti, Earthquake damages to cultural heritage constructions and simplified assessment of artworks, Engineering Failure Analysis, v. 34, (2013), pp. 735-760.

[28] N. Augenti, F. Parisi, Learning from construction failures due to the 2009 L'Aquila, Italy, earthquake, J Perform ConstrFacil, v. 24 (6), (2010), pp. 536-555.

[29] A. Maria D'Altri, G. Castellazzi, S. de Miranda, A. Tralli, Seismic-induced damage in historical masonry vaults: A case-study in the 2012 Emilia earthquake-stricken area, Journal of Building Engineering, v. 13, (2017), pp. 224-243.

[30] G. Croci, The Basilica of St. Francis of Assisi after the September 1997 earthquake, Struct. Eng. Int., v. 8 (1), (1998), pp. 56-58.
[31] B. Sáez Riquelme, S. Iglesias Salón Valencianas XVIII. Levantamiento gráfico, análisis geométrico y constructivo, patología común. (Ph.D thesis). Departamento de Sistemas Industriales y Diseño. Universitat Jaume I, Castellón (Spain), 2013. n.d.
[32] https://www.mapei.com/it/en/products-and-solutions/products/detail/mapegrid-g-220
[33] https://www.mapei.com/it/en/products-and-solutions/products/detail/planitop-hdm-restauro
[34] T. Rotunno, M. Fagone, E. Bertolesi, E. Grande, G. Milani, Curved masonry pillars reinforced with anchored CFRP sheets: An experimental analysis, Composites Part B: Engineering, v. 174, (2019), pp. 107;